MNK Publication

International Journal of Latest Research in Science and Technology **ISSN (Online):2278-5299**
Volume 4, Issue 6: Page No.29-38, November-December 2015
https://www.mnkpublication.com/journal/ijlrst/index.php

MATHEMATICAL MODELING APPROACH FOR DETERMINING TYPE-1 LOAD-FLOW SOLUTIONS OF POWER SYSTEMS

Chen-Sung Chang
Department of Information Management, Nan-Kai University of Technology, Nantou County, Taiwan

Abstract*- *A mathematical modeling approach based on the continuation power flow (CPFLOW) analysis method is proposed for locating the Type-1 load-flow solutions of a power system. Importantly, the proposed method enables all of the Type-1 load-flow solutions to be obtained by tracing just a small number of homotopy curves. The validity of the proposed approach is demonstrated using 5-bus and 7-bus power systems for illustration purposes. The results show that the proposed method not only has the ability to locate all of the Type-1 load-flow solutions, but also has a lower computational complexity than existing schemes.

Keywords - Type-1 solutions; Continuation power flow (CPFLOW) analysis; Stable equilibrium point (SEP); Manifold

I. INTRODUCTION

Voltage instability is one of the leading causes of network collapse worldwide [1]-[3], and has therefore attracted significant attention in the literature. It was shown in [4] that the voltage collapse phenomenon is associated with the nonlinearity of the load-flow equations, which results in multiple potential load-flow solutions. Various methods have been proposed for determining the voltage stability limits of power networks using load-flow analysis techniques [5]-[8]. For example, the authors in [6]-[8] evaluated the voltage stability limit by inspecting the distance between the operable load-flow solution and an appropriate low-voltage load-flow solution.

The literature contains many proposals for identifying some (or all) of the load-flow solutions for a power system [9]-[14]. In [9], a special probability-one homotopy method was tailored to find all the load-flow equations of 5-bus and 7-bus systems. However, the proposed method requires the tracing of a large number of homotopy curves, and is therefore computationally intensive. In [10], the authors proposed a algorithm to locate all the load-flow solutions by tracing a large number of homotopy curves. However, the method is computationally complex, and is therefore feasible only for small-scale power systems. Furthermore, while both methods in [9] and [10] have the ability to locate all of the load-flow solutions, the relationship between these solutions and the voltage stability of the power system is unclear.

In the power systems field, a Type-1 solution simply means that the Jacobian matrix of the load-flow solution set has exactly one eigenvalue with a positive real part, while the remainder of the eigenvalues have negative real parts. In general, a solution is considered to be Type-k when there exist k positive values for the real parts of the eigenvalues, where these eigenvalues can be either complex numbers or real numbers. It was shown theoretically in [11] and [12] that only Type-1 load-flow solutions are associated with the voltage instability phenomenon. Thus, it is reasonable to infer that the task of identifying the voltage stability properties of a power system can be simplified by searching for only the Type-1 load-flow solutions. Accordingly, several methods have been proposed for solving Type-1 load-flow problems [13] [14] [15]. However, these methods do not guarantee the discovery of all the Type-1 solutions.

To address this problem, the present group previously proposed a method for identifying all of the Type-1 solutions for a power network using a continuation power flow (CPFLOW)-based algorithm [16]. The present study performs a systematic theoretical analysis of the proposed method and compares its performance with that of two existing methods [9] [10]. It is shown that the proposed method not only has the ability to identify the complete set of Type-1 solutions, but also has a significantly lower computational complexity than existing methods. The remainder of this paper is organized as follows. Section 2 formulates the load-flow equations and solution manifolds. Section 3 describes the manifold-tracing method used by the CPFLOW algorithm to locate all of the Type-1 load-flow solutions. Section 4 presents and discusses the simulation results. Finally, Section 5 provides some brief concluding remarks.

II. MATHEMATICAL MODELING OF LOAD-FLOW EQUATIONS AND SOLUTION MANIFOLDS

The load-flow problem may now be stated with some precision. The formulation is based on operational considerations of the power industry as well as mathematical considerations. We will dicuss some of these considerations and terminology.

Some buses are supplied by generators; we can call these generator buses. Bus 1 is called a slack bus or swing bus; the other generator buses are called PV buses. Other buses without generator s are called load buses or PQ buses. We consider a power system S with N buses, including m PV buses and a slack bus, n PQ buses,. Let $V=[v_1,v_2,\cdots,v_n]$, $\theta_q=[\theta_1,\theta_2,\cdots,\theta_n]$ be the vectors

Publication History
Manuscript Received : *3 December 2015*
Manuscript Accepted : *16 December 2015*
Revision Received : *26 December 2015*
Manuscript Published : *31 December 2015*

of the bus voltages and bus angles on the PQ buses, respectively. Furthermore, let $\theta_v = [\theta_1, \theta_2, \cdots, \theta_m]$, $Q_v = [q_1, q_2, \cdots, q_m]$ be the vectors of the bus voltages and reactive power on the PV buses, respectively. The real and reactive power balance equations of the PQ buses can be written in the following vector forms:

$$f_p(V, \theta_q, \theta_v) - P = 0 \tag{1}$$

$$f_q(V, \theta_q, \theta_v) - Q = 0 \tag{2}$$

where P and Q are the real and reactive bus powers of the PQ buses, respectively. Similarly, the real and reactive power balance equations of the generator buses can be expressed as

$$f_{pv}(V, \theta_q, \theta_v) - P_v = 0 \tag{3}$$

$$f_{qv}(V, \theta_q, \theta_v) - Q_v = 0 \tag{4}$$

Where P_v is the real bus power of the PV buses.

Let the following assumption be made.

Assumption 1: At least one of the solutions to the load-power equations is known.

Note that this assumption is reasonable given the extensive attention paid to the load-flow problem by the power systems community in recent decades. Moreover, if not even one solution for the load-power equations can be found, there is little point in searching for "other" solution points.

In performing a load-flow study, the aim is to find a suitable operating point for the power system, i.e., an operating point which ensures that the system satisfies all of the specified operational constraints (e.g., a limited generator reactor power capability, the voltage mainitude bounds, and so on.) Having found such an operating point, the next step is to find all of the other solutions to the same system. Notably, all of these solutions should satisfy the same load-flow equation as the original solution, and hence their implementation should require no further adjustments to be made to the system. Furthermore, since the power system is not actually expected to operate at these subsequent solutions, the operational limits bear no significance to them. That is, given an interest in a particular solution, one can easily invoke a load-flow study at this solution point, after all the solutions have been found, in order to check if it represents a suitable operating point. Hence, the following assumption can be made:

Assumption 2: No reactive power limit is imposed on the PV buses when solving for other solutions.

Note that Assumption 2 allows the dimension of the load-flow equations to be reduced. In addition, it is noted in Eq. (4) that the unknown Q_v is separated from the other unknown variables, and does not appear in any other equation. As a result, Eq. (4) imposes no constraint on the other unknown variables, and can therefore be removed when solving for them. Accordingly, in the following discussions, Q_v is excluded from the unknowns and Eq. (4) is removed from the formulations. Hence, the load-flow equations comprise only Eqs. (l), (2) and (3). Let the number of unknowns be equal to $K = 2n + m$, and write the unknown variables, V , θ_q and θ_v , into a single K-dimensional vector x, i.e., $x = [V, \theta]^T$. Thus we first consider the load-flow equation defined as:

$$P_i(x) - P_i = 0, \qquad i = 2, \cdots, N \tag{5}$$

$$Q_i(x) - Q_i = 0, \quad i = m + 2, \cdots, N \tag{6}$$

where N is the total number of buses including slack bus, m is the total number of PV buses excluding slack bus. The state variables x is represented as vector $[V, \theta]^T$.

Let α_{pi} and α_{qi} be parameter vectors, load parameters α_{pi} indicate the variations of the active power of PV buses and PQ buses, and load parameters α_{qi} indicate the variations of the reactive power of PQ buses. The α_{pi} and α_{qi} vectors can be added to Eqs. (5) and (6), respectively, to form the following compact-form parameterized load-flow equation:

$$F(x, \alpha) = f(x) + \alpha = \begin{bmatrix} P_2(x) - P_2 + \alpha_{p2} \\ \vdots \\ P_N(x) - P_N + \alpha_{pN} \\ Q_{m+2}(x) - Q_{m+2} + \alpha_{q(m+2)} \\ \vdots \\ Q_N(x) - Q_N + \alpha_{qN} \end{bmatrix} = 0 \tag{7}$$

where $\alpha = [\alpha_{pi}, \alpha_{qi}]^T \in \Re^K$, and F : $D \times \Re^K \to \Re^K$ is a smooth function.

From an engineering point of view, load-flow solutions sensitive to small changes in the system parameters bear no significance. Hence, the following assumption can be made:

Assumption 3: All of the solutions to the load-power equation are structurally stable.

In other words, all of the solutions persist under small perturbations. Mathematically, this means that all of the solutions are isolated solutions.

It is noted that the parameterized load-power equation

$$F(x, \alpha) = 0 \tag{8}$$

is a smooth function. The K equations in $2K$ variables define an K -dimensional manifold in a $2K$ -dimensional space. Setting $\alpha = 0$ yields

$$F(x, 0) = f(x) + 0 = f(x) = 0 \tag{9}$$

That is, the solutions to the load-flow equation (Eq. (5) and Eq. (6)) are embedded in the manifold and can therefore be derived from this manifold given a suitable processing approach. However, dealing with a high-dimensional manifold is difficult to deal with efficiently by computers involves a high computational complexity. Thus, for convenience, the present analysis considers only a very small region of this manifold by re-formulating the parameterized load-flow equation given in (7) as follows:

$$F_i(x,\alpha_i) = f(x) + \begin{bmatrix} 0 \\ \vdots \\ \alpha_i \\ \vdots \\ 0 \end{bmatrix} = 0 \quad (10)$$

Note that the superscript i in the term F_i indicates that the equation is associated with the i-th parameter α_i in vector α. The same notation is applied in determining the solution set M_i of Eq. (10). Let the following lemma be introduced:

Lemma 1: Generically, the solution set of Eq. (10), i.e.,

$$M_i = \{(x,\alpha_i) \mid F_i(x,\alpha_i) = 0\} \quad (11)$$

is a one-dimensional manifold.

This manifold consists of components which do not intersect one another. Thus, the following lemma can also be given:

Lemma 2: Generically, manifold M_i is a disjoint union of connected components C_i^k, i.e.,

$$M_i = \bigcup_{set\ of\ k} C_i^k \quad (12)$$

Collectively, Lemma 1 and 2 indicate that the solution set M_i of Eq. (10) comprises a bunch of several smooth, one-dimensional curves, C_i^k, which neither intersect one another nor themselves. In the event that M_i violates the said characterizations, the following arbitrarily small perturbation can be applied to achieve compliance:

$$F_i(x,\alpha_i) + \varepsilon = 0 \quad (13)$$

Note that this perturbation amounts to perturbing the assigned bus power injections, P *and* Q, while leaving the basic structure of the load-flow equation unchanged.

For manifold M_i, the following important topological characteristic applies:

Theorem 1: The solution manifold M_i of equation $F_i(x,\alpha_i) = 0$ is bounded.

In practice, changing parameter α_i amounts to changing the real or reactive power on one bus. In other words, Theorem 1 simply states that if all of the other bus powers remain unchanged, the capability of the network to transfer power (real or reactive) to or from a single bus is limited.

According to the Classification Theorem of Compact Manifold [17], a compact one-dimensional manifold is topologically equivalent to either a circle or a closed interval. From Lemma 1, it will be recalled that M_i comprises a set of one-dimensional curves, C_i^k. Moreover, Theorem 1 states that M_i (and hence C_i^k') are bounded. In other words, they are compact one-manifolds. Since curve C_i^k has no endpoint, it cannot be topologically equivalent to a closed interval. Therefore, the following proposition holds.

Lemma 3: Each one-dimensional curve C_i^k of M_i is topologically equivalent to a circle S^1.

That is, each component C_i^k of M_i is a smooth one-dimensional curve in the shape of an endless loop. And each M_i retains the whole solution set of the load-power equation given in Eq. (5) and Eq. (6). In other words, from Eq. (10), setting $\alpha_i = 0$ yields the load-flow equation (Eq. (5) and Eq. (6)).

Lemma 4: Generically, each solution point to Eq. (7) is connected to at least one other solution point via a one-dimensional curve C_i^k of manifold M_i.

This can be confirmed by verifying that the solutions of Eq.(8) is located at the intersection of manifold M_i with the hyperplane

$$H_{\alpha_i} = \{(x,\alpha_i) \in D \times \Re \mid \alpha_i = 0\} \quad (14)$$

Generically, an endless loop C_i^k will intersect this hyperplane at an even number of points. Therefore, for each solution point at the intersection of C_i^k and H_{α_i} there exists at least one other solution point where C_i^k intersects H_{α_i}. The following theorem can be defined:

Theorem 2: If all of the elements in vectors P and Q are non-zero (note that the zero elements can be perturbed by an arbitrary small constant in order to make them non-zero, if necessary), and all of the voltage magnitudes are positive at one point on curve C_i^k, then the voltage magnitudes are positive everywhere on curve C_i^k.

The following discussions focus on *one-dimensional curve C_i^k of manifold M_i* and assume that all of the voltage variables have a positive magnitude. And assume that the load-flow equation has *t* solutions. The number t is unknown until all the solutions has been found, by tracing all the one-dimensional manifolds, M_i, $i = 2,\cdots,N$, we can locate all the solutions. In other words, any solution of the load-power equation is reachable from all of the other solutions via the manifolds M_i, $i = 2,\cdots,N$. If the manifolds corresponding to parameters α_{pi} form a connected graph. The same inference also holds true for the manifolds corresponding to parameters α_{qi}. Notably, Theorem 2 also implies that any solution of Eq. (7) can reach all of the other solutions via manifolds $M_i, \forall i$

III.MANIFOLD-TRACING METHOD FOR LOCATING TYPE-1 SOLUTIONS

Let the power system be modeled as the following differential equation with a vector α of slowly varying parameters, i.e.,

$$\dot{x} = F(x,\alpha), \quad x \in \Re^K, \quad \alpha \in \Re^K \quad (15)$$

where x is a state vector which includes both the bus voltage magnitudes and the angles, and α is a vector of the real and reactive load powers. An assumption is made that $F:\Re^K \to \Re^K$ satisfies the conditions required to ensure the existence and uniqueness of the solutions. Moreover, a point on the manifold curve is said to be an equilibrium point of Eq. (15) if $F(x_0,\alpha)=0$. The equilibrium point x_0 is "hyperbolic" if the Jacobian matrix $D_xF(x_0,\alpha)$ has no eigenvalues with zero real parts, and is said to be "simple" if the determinant of $D_xF(x_0,\alpha)$ is non-zero. Finally, the "Type" of the hyperbolic equilibrium point x_0 is defined as the number of eigenvalues of $D_xF(x_0,\alpha)$ which have a positive real part.

The unstable manifold $M^u(x_0)$ (stable manifold $M^s(x_0)$) of an equilibrium point x_0 is the manifold in the state-space form whose trajectories converge to x_0 as $t\to-\infty$ ($t\to\infty$) and which is tangent at x_0 to the subspace spanned by the eigenvectors associated with eigenvalues with positive (negative) real-parts. If x_0 is hyperbolic, the dimension of $M^u(x_0)$ is equal to the "Type" of x_0.

In general, the load of a power network varies with time. Consequently, α is a function of time t and Eq. (15) can be regarded as a differential equation parameterized by the single parameter t. That is,

$$\dot{x}=F(x,\alpha(t)),\quad x\in\Re^K,\quad t\in\Re \qquad (16)$$

where x is an K-dimensional state vector and α is a time-varying parameter. The system in Eq. (16) can be approximated using the following assumption:

Assumption 4: α varies quasistatically.

That is, α varies sufficiently slowly that the system in Eq. (16) can be well approximated by keeping α constant whileleaving the other system dynamics unchanged.

Assumption 5: The system in Eq. (18) is in the generic set of systems S_1.

Note that S_1 is a generic set of systems described by Sotomayor [18], and consists of systems of the form shown in Eq. (16), which (for each α) all have simple equilibria although one of the equilibria may be a non-degenerate saddle node equilibrium.

Lemma 5: Suppose that the system given in Eq. (16) satisfies Assumption 6. Consequently, the only way in which a stable equilibrium point $x_0(\alpha)$ can disappear is via the coalescence with a Type-1 equilibrium point $x_1(\alpha)$ at a saddle-node bifurcation, where $x_1(\alpha)$ is on the stability boundary $x_0(\alpha)$ and $x_1(\alpha)$ is the closest unstable equilibrium point to $x_0(\alpha)$ [19].

Typically, there are two ways in which a stable equilibrium point can lose stability, namely it can disappear as stated in Lemma 5 above or it can persist but become unstable by interacting with a limit cycle in a Hopf bifurcation [19]-[21]. Lemma 5 does not exclude Hopf bifurcations. However, many power system models do not admit limit cycles, and therefore cannot have Hopf bifurcations.

When an equilibrium point $x_0(\alpha)$ is stable, it lies in the interior of its stability region. As a result, $x_0(\alpha)$ can only disappear by bifurcating with an equilibrium point $x_1(\alpha)$ on its stability boundary. Lemma 5 states that $x_1(\alpha)$ must therefore be Type-1 and its unstable manifold $M^u[x_1(\alpha)]$ one-dimensional. $M^u[x_1(\alpha)]$ may thus be decomposed as

$$M^u[x_1(\alpha)]=M_-^u\cup\{x_1(\alpha)\}\cup M_+^u \qquad (17)$$

where M_-^u lies inside the stability region of $x_1(\alpha)$ and joins $x_0(\alpha)$ to $x_1(\alpha)$, while M_+^u lies outside the stability region of $x_0(\alpha)$.

At the bifurcation point, $\alpha=\alpha^*$, $x_0(\alpha)$ and $x_1(\alpha)$ coalesce to form the equilibrium point $x^*=x_0(\alpha^*)=x_1(\alpha^*)$. The Jacobian matrix at x^* has a zero eigenvalue associated with an eigenvector v in the direction in which $x_0(\alpha)$ and $x_1(\alpha)$ coalesced. The other eigenvalues of the Jacobian matrix have negative values. Therefore, x^* has a one-dimensional center manifold M^c and an $K-1$ dimensional stable manifold $M^s(x^*)$. M^c can be decomposed as

$$M^c=M_-^c\cup\{x^*\}\cup M_-^c \qquad (18)$$

and v is tangent to M^c at x^*. The vector field at x^* has one-sided stability along M^c. Moreover, x^* is stable along M_-^c and unstable along M_+^c, where M_+^c is a unique system trajectory. Note that M_+^u becomes M_+^c when bifurcation occurs.

Based on the discussions above, the following models for voltage collapse before and after saddle node bifurcation, repectively, can be proposed.

Model 1

Before bifurcation, the system has a stable equilibrium point x_0 and all the eigenvalues of the Jacobian matrix $D_xF(x_0,\alpha)$ have negative real parts. As parameter α slowly varies, the stable equilibrium point x_0 also varies and the system state x tracks x_0. In other words, x_0 is not only a stable equilibrium point, but also the system operating point. Thus, a static (or quasistatic) model $0=F(x,\alpha)$ can be used prior to bifurcation.

Model 2

After bifurcation, x^* is unstable and the system dynamics can be approximated by the system state moving along trajectory M_+^c, i.e., the unstable part of the center manifold of x^*. If M_+^c points in such a direction in the state space that the voltage magnitudes decrease as the system state moves along M_+^c, then voltage collapse can be identified with movement along M_+^c.

Let $\alpha^* = \alpha(t_*)$ be the critical value of the parameter vector at the bifurcation point and let x^* denote the corresponding equilibrium point formed by the coalescence of x_0 and x. The Jacobian matrix $D_x F(x^*, \alpha^*)$ is singular and has a unique simple zero eigenvalue with a corresponding right eigenvector v^* such that

$$D_x F(x^*, \alpha^*) v^* = 0 \tag{19}$$

where v^* is the direction in state space of the initial voltage collapse dynamics. It is noted that v^* is tangent to M_+^c at x^*. Moreover, any of the state variables can collapse as the system dynamics move in direction v^*.

As well as defining the direction of the initial voltage collapse dynamics, v^* also provides a useful interpretation role in the static model $0 = F(x, \alpha)$. Specifically, when bifurcation occurs, the equilibria x_0 and x coalesce and v^* indicates the asymptotic direction in which x_0 and x approach one another. Note that this can be proven via the Liapunov-Schmidt reduction [22], which completely solves the local geometry of $0 = F(x, \alpha)$ near (x^*, α^*).

Near a saddle node bifurcation (i.e., α near α^*), x_1 is near x_0 and $D_x F(x_0, \alpha)$ has a unique, simple negative eigenvalue w of smallest absolute magnitude and a corresponding right eigenvector v. Furthermore, $w \to 0$ and $v \to v^*$ as $\alpha \to \alpha^*$. Since v is a continuous function of α, v lies approximately along the line joining x_0 and x_1 when the system is close to bifurcation. Thus, given x_0, the best estimate for the direction in which to find x_1 is given by v or $-v$. This observation is useful since one can then choose initial conditions for the numerical calculation of the Type-1 solutions along the line passing through the x_0 stable equilibrium point (SEP) in the direction of the function of α.

Based on the principles described above, this study uses a CPFLOW analysis technique to search for all of the Type-1 load-flow solutions by varying one load parameter, α_{pi} or α_{qi}, for each trace and passing through all of the PV and PQ buses.

The CPFLOW analysis technique uses continuation methods to trace power system behavior due to load and generation variation. The theory of continuation methods has been studied extensively and has its roots in Algebraic Topology and Differential Topology [23]-[25]. The CPFLOW analysis is based on the following three elements to solution as one parameter in the compact-form parameterized load-flow equation (7) varies each time.

Continuation parameter element: Every continuation method has a particular parameterization scheme (i.e., physical parameterization, local parameterization or arclength parameterization). The parameterization offers a way of identifying each solution in the manifold so that the "previous" solution or "next" solution can be quantified. The scheme of choosing the continuation parameter used in this paper is the local parameter, which uses either the load parameter (α_{pi} or α_{qi}) or any component of the state vector x to parameterize the solution curve of Eq. (7). The step length in the local parameterization is $\Delta\alpha$ or Δx.

Predictor element: The purpose of the predictor is to find an approximation point for the next solution. Suppose we are at the i-th step of the the continuation process and the i-th solution (x^i, α^i) of Eq. (7) has been found. The predictor attempts to find an approximation point for the next solution (x^{i+1}, α^{i+1}). The quality of the approximation point by a predictor significantly affects the number of iterations required by a corrector inorder to obtain an exact solution.

Once a base stable solution point has been found by flat start, the prediction of the next solution can be made by taking an appropriate step size in the tangent direction of the manifold. Therefore, the task in the predictor process is to calculate the tangent vector. The tangent vector calculation is derived by taking the derivative of both sides of the equation (7) and presented in matrix form as

$$\begin{bmatrix} \frac{\partial F}{\partial x} & \frac{\partial F}{\partial \alpha} \end{bmatrix} \begin{bmatrix} dx & d\alpha \end{bmatrix}^T = 0 \tag{20}$$

where $\begin{bmatrix} \frac{\partial F}{\partial x} & \frac{\partial F}{\partial \alpha} \end{bmatrix}$ is the conventional load flow Jacobian augmented by one column $\partial F / \partial \alpha$ and the number of equations remains unchanged. Thus, one more equation is needed. This problem can be solved by choosing a non-zero magnitude (say one) for one of the components of the tangent vector, and the tangent vector is defined as $\hat{t} = [dx, d\alpha]^T$, and $\hat{t}_i$ is equal to +1 or –1 depending on how the i-th state variable variations as the solution curve is being traced. If it increases, then the +1 should be used, otherwise the –1 is used. Therefore, one equation is added to equation (20) and the equation can be modified as

$$\begin{bmatrix} \frac{\partial F}{\partial x} & \frac{\partial F}{\partial \alpha} \\ E_i & \end{bmatrix} \hat{t} = \begin{bmatrix} 0 \\ \pm 1 \end{bmatrix} \tag{21}$$

where E_i is a row vector with all elements equal to zero except the i-th element which equals one. $\hat{t}$ has a non-zero

norm such that the augmented Jacobian will be nonsingular at the saddle-node bifurcation point.

A predictor, known as the tangent predictor, uses a first-order polynomial (a straight line) passing through the current and previous solutions to predict the next solution. And if the tangent vector has been found by equation (21), then the predicted point could be written as

$$(\tilde{x}^{i+1}, \tilde{\alpha}^{i+1}) = (x^i, \alpha^i) + h(dx, d\alpha) \quad (22)$$

where "~" denotes the predicted solution, and h is an appropriate step-size. h is one key element of affecting the computational efficiency of continuation methods. Ideally, the h should be adapted to the shape of the solution curve to be traced: a larger step length should be used in the 'flat' part of the solution curve and a smaller step-length in the 'curly' part (part with high degree of curvature) of the solution curve.

Corrector element: Once a predicted solution of the manifolds has been found, and the error must be corrected. Thus a good predictor gives an approximate solution, $(\tilde{x}, \tilde{\alpha})$, which is in the neighborhood of the next solution, $(\bar{x}, \bar{\alpha})$. So a few iterations is used as the corrector element for achieve the accurate solution. The Newton-Raphson method is chosen as the corrector. This choice has an advantage that the existing load flow computer package based on the Newton-Raphson method can be utilized. And the accurate point can be expressed as

$$(\bar{x}, \bar{\alpha}) = (\tilde{x}, \tilde{\alpha}) + (\Delta x, \Delta\alpha) \quad (23)$$

where $(\Delta x, \Delta\alpha)$ is found by Newton-Raphson iterations.

IV. TEST AND RESULTS

In this section, the validity of the methodolgy proposed in Section 3 is demonstrated by locating all of the Type-1 solutions for the 5- and 7-bus power systems considered in a previous study by the current group [16]. The two test examples (5-bus and 7-bus systems) are chosen because all load flow solutions have been calculated in [9] and [10]. They also serve as a basis for the comparison between different methods.

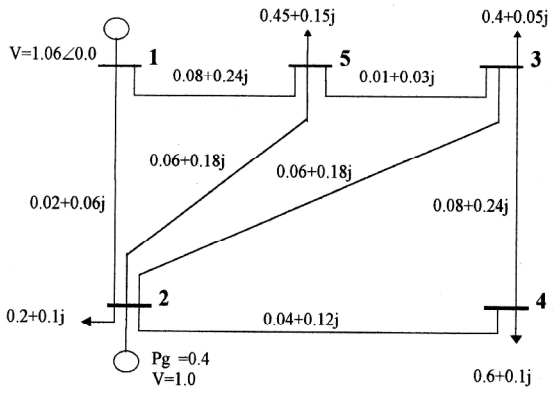

Fig. 1 The 5-bus system

Figure 1 presents the one-line diagram of the 5-bus system (Note that Bus 1 is the slack bus). Table 1 shows the four Type-1 load-flow solutions found for the system.

The Jacobian eigenvalues of the Type-1 solutions are listed in Table 2. It is noted that the eigenvalues of the Jacobian matrix for the Type-1 load-flow solutions have a single positive real part, while the other eigenvalues have a negative real part.

Comparing our results with reference [9] and [10], it is clear that all searched Type-1 load flow solutions in the 5-bus system by the proposed CPFLOW-based method are complete. The CPFLOW manifold tracing process for the 5-bus system is summarized in Table 3. As shown, the process commenced by selecting the variations of the active power of Bus 2, and treating the variations of the reactive powers of Buses 3, 4 and 5, respectively, as continuation parameters at the beginning of each trace. Moreover, the flat point in the manifold was taken as the initial state in searching for the stable equilibrium point.

TABLE 1 THE FOUR TYPE-1 LOAD FLOW SOLUTIONS OF THE 5-BUS SYSTEM

Variables	Solutions			
	1	**2**	**3**	**4**
θ_1	0.000000	0.000000	0.000000	0.000000
θ_2	-138.967855	-16.503994	-12.146784	-16.908807
θ_3	-134.863861	-81.865310	-13.879429	-37.786156
θ_4	-141.660453	-23.451893	-71.501631	-23.872760
θ_5	-129.850916	-26.042191	-12.679258	-69.041445
V_1	1.060000	1.060000	1.060000	1.060000
V_2	1.000000	1.000000	1.000000	1.000000
V_3	0.587894	0.030137	0.740259	0.184600
V_4	0.831660	0.628869	0.057975	0.686517
V_5	0.501169	0.197185	0.793300	0.034177

TABLE 2 THE JACOBIAN EIGENVALUES OF TYPE-1 SOLUTIONS FOR THE 5-BUS SYSTEM. (EIGENVALUES WITH POSITIVE REAL PARTS ARE CIRCLED.)

	Solution Number			
	1	**2**	**3**	**4**
Eigenvalue	-29.1332+4.2405j	-20.7505	-46.6051+14.1799j	-21.3485
	-29.1332-4.2405j	2.7585	-46.6051-14.1799j	4.7062
	7.9327	-1.1522	-23.7529	-8.3728
	-9.9385+3.1723j	-3.7614	3.1191	-4.4286
	-9.9385-3.1723j	-7.1770	-6.2482	-0.9235
	-4.0537+1.5817j	-6.7345	-4.5908	-1.6543
	-4.0537-1.5817j	-2.5251	-1.8625	-6.4539

TABLE 3 MANIFOLD TRACING PROCESS FOR 5-BUS SYSTEM

Load Parameter	P2+	P2-	Q3+	Q3-	Q4+	Q4-	Q5+	Q5-
Solution Number	1	1	2	1	3	1	4	1

The first row in Table 3 shows the load bus used in tracing the corresponding Type-1 solutions. The "+" sign indicates that the search process takes place in the direction of increasing load parameters at the beginning of the manifold, while the "-" sign indicates that the search process takes place in the direction of decreasing load parameters. The second row in the table shows the sequence in which the traces were performed.

Figures 2(a) and 2(b) show the manifolds of the first two traces for solution number 1 in the $\alpha_{P2} - V_5$ plane. The remaining manifolds are shown in Figs. 3 ~ 5.

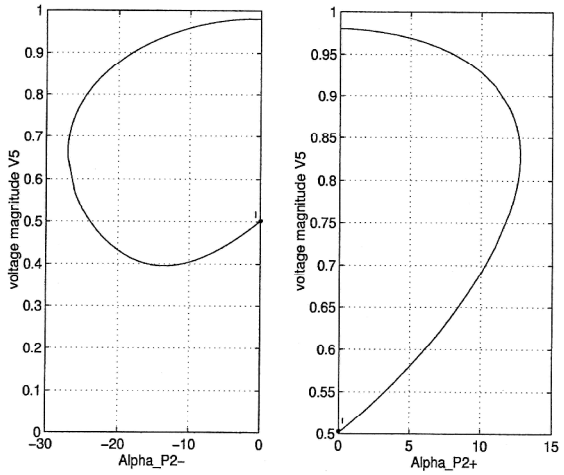

(b) $\alpha_{P2-} - V_5$ plane (a) $\alpha_{P2+} - V_5$ plane

Fig. 2 Manifold of first trace in $\alpha_{P2} - V_5$ plane

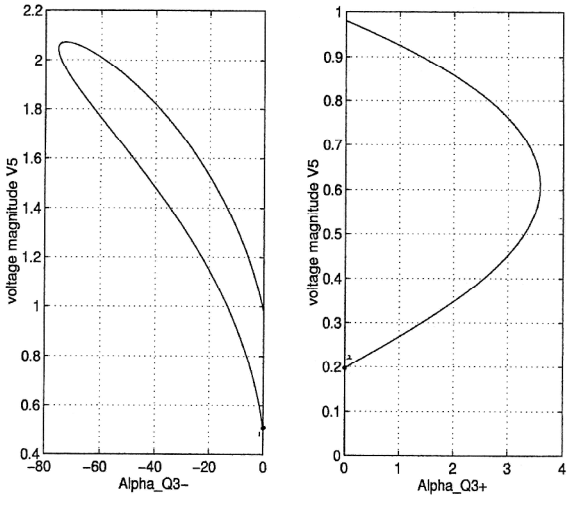

(b) $\alpha_{q3-} - V_5$ plane (a) $\alpha_{q3+} - V_5$ plane

Fig. 3 Manifold of first trace in $\alpha_{q3} - V_5$ plane

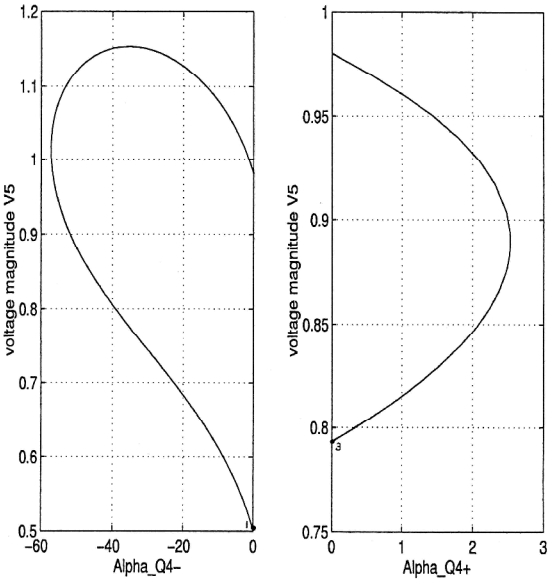

(b) $\alpha_{q4-} - V_5$ plane (a) $\alpha_{q4+} - V_5$ plane

Fig. 4 Manifold of first trace in $\alpha_{q4} - V_5$ plane

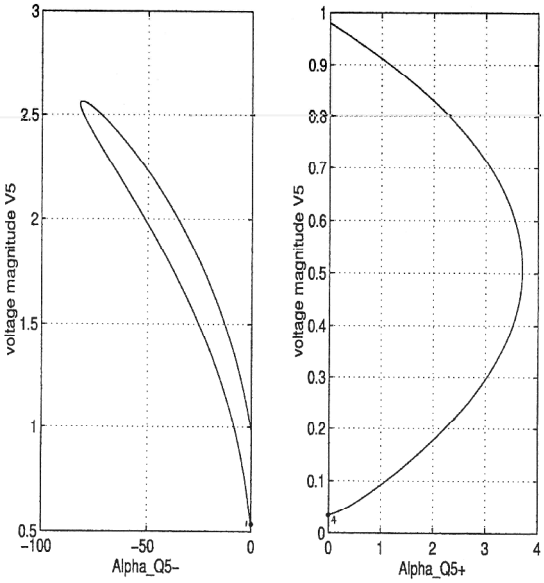

(b) $\alpha_{q5-} - V_5$ plane (a) $\alpha_{q5+} - V_5$ plane

Fig. 5 Manifold of first trace in $\alpha_{q5} - V_5$ plane

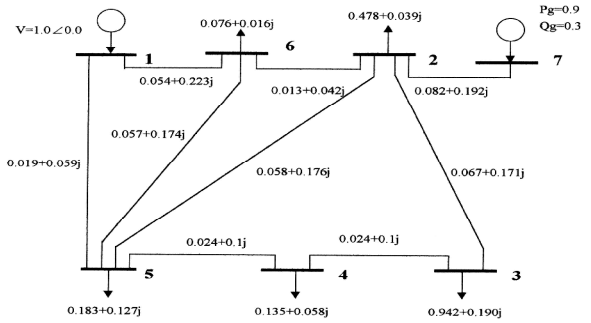

Fig. 6 The 7-bus system

Figure 6 shows the one-line diagram of the 7-bus system (Note that Bus 1 is again taken as the slack bus). Table 4 shows the two Type-1 load flow solutions found for the system. Meanwhile, Table 5 shows the Jacobian matrix eigenvalues of the Type-1 solutions. As in the previous example, the eigenvalues of the Jacobian matrix for the Type-1 load flow solutions have a single positive real part, while the remaining eivenvalues have a negative real part. Finally, Table 6 shows the manifold tracing process for the 7-bus system.

TABLE 4 THE TWO TYPE-1 LOAD FLOW SOLUTIONS OF THE 7-BUS SYSTEM

Variables	Solutions		Variables	Solutions	
	1	2		1	2
θ_1	0.000000	0.000000	V_1	1.000000	1.000000
θ_2	-5.221185	-6.293491	V_2	0.587562	0.541465
θ_3	-52.677524	-19.809837	V_3	0.174508	0.543027
θ_4	-14.205551	-11.246364	V_4	0.412175	0.645773
θ_5	-3.205593	-3.861835	V_5	0.722940	0.775000
θ_6	-4.303086	-5.016062	V_6	0.663768	0.640149
θ_7	14.957620	101.82011	V_7	0.731202	0.287970

TABLE 5 THE JACOBIAN EIGENVALUES OF TYPE-1 SOLUTIONS FOR THE 7-BUS SYSTEM. (EIGENVALUES WITH POSITIVE REAL PARTS ARE CIRCLED.)

	Solution Number	
	1	2
Eigenvalue	-28.2369+5.8497j	-26.0601+4.3956j
	-28.2369-5.8497j	-26.0601-4.3956j
	-23.7162+5.7252j	-27.0596+6.9031j
	-23.7162-5.7252j	-27.0596-6.9031j
	-6.1334+1.5566j	-11.2898+1.3657j
	-6.1334-1.5566j	-11.2898-1.3657j
	-6.7628	0.9611
	1.8125	-5.9566+1.3536j
	-2.4340	-5.9566-1.3536j
	-1.0813	-0.9947
	-1.8035	-1.8087
	-4.2080	-3.1520

TABLE 6 MANIFOLD TRACING PROCESS FOR 7-BUS SYSTEM

Load Parameter	P2+	P2-	P3+	P3-	P4+	P4-	P5+	P5-	P6+	P6-	P7+	P7-
Solution Number	1	1	1	1	1	1	1	1	1	1	2	2

As shown in Table 6, the Type-1 solutions for the 7-bus system were identified by selecting the variation of the active powers of Buses P2, P3, P4, P5, P6 and P7, respectively, at the beginning of each tracing process. Figures 7(a) and 7(b) show the manifolds of the first two traces of the first solution in the $\alpha_{P2} - V_3$ plane for Bus 2 in the 7-bus system. Figures 8~12 show the traced manifolds for Buses 3, 4, 5, 6 and 7, respectively. And comparing our results with reference [9] and [10], it is clear that all searched Type-1 load flow solutions in the 7-bus system by the proposed CPFLOW-based method are complete.

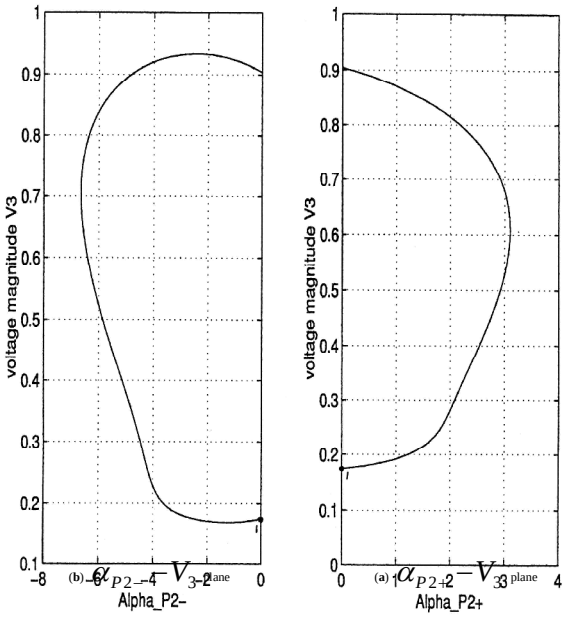

Fig. 7 Manifold of first trace in $\alpha_{P2} - V_3$ plane

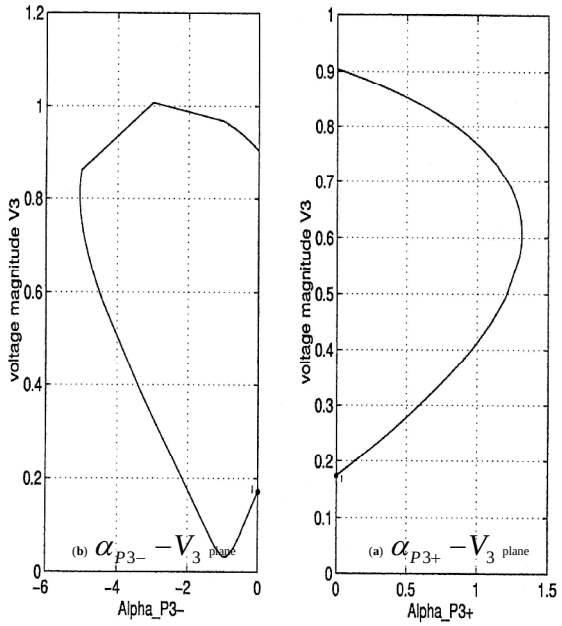

Fig. 8 Manifold of first trace in $\alpha_{P3} - V_3$ plane

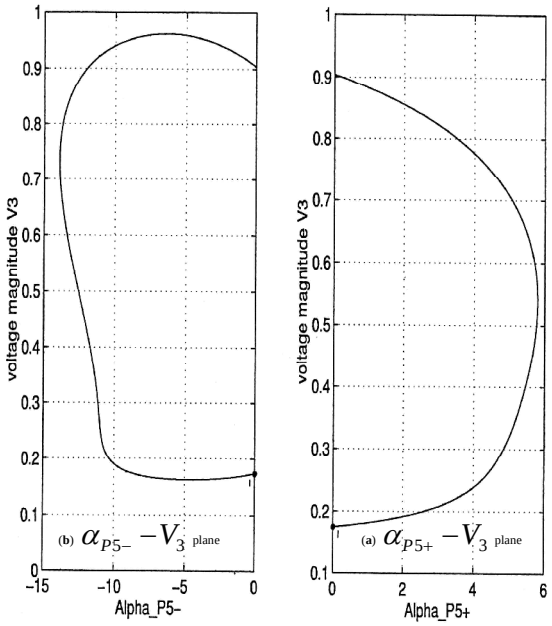

Fig. 10 Manifold of first trace in $\alpha_{P5} - V_3$ plane

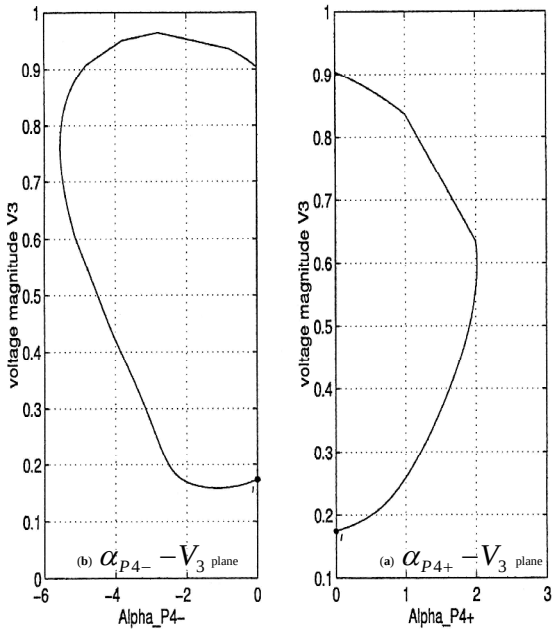

Fig. 9 Manifold of first trace in $\alpha_{P4} - V_3$ plane

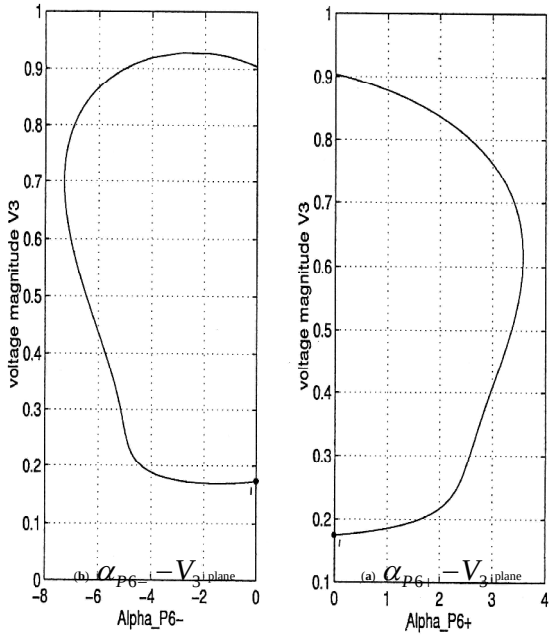

Fig. 11 Manifold of first trace in $\alpha_{P6} - V_3$ plane

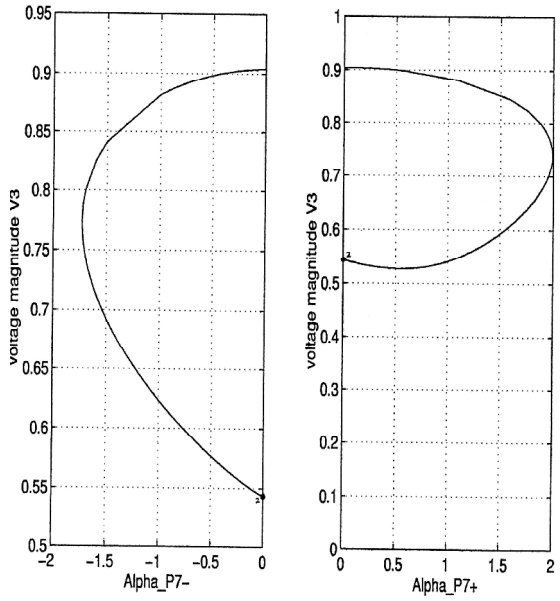

(b) $\alpha_{P7-} - V_3$ plane (a) $\alpha_{P7+} - V_3$ plane

Fig. 12 Manifold of first trace in $\alpha_{P7} - V_3$ plane

The test results indicate that we only to traces 4 and 5 manifolds for the 5- and 7-bus power systems to find all of the type-1 load flow solutions by CPFLOW-based method, and void the fractal phenomenon.

V. CONCLUSIONS

This study has performed a theoretical analysis of the CPFLOW-based algorithm proposed in a previous study [16] to identify all of the Type-1 load-flow solutions for a power system. It has been shown that the proposed method enables the complete set of Type-1 solutions to be identified by tracing a smaller number of manifolds than the methods proposed in [9] and [10], respectively. Specifically, the proposed method requires the tracing of just $2(N-1)$ manifolds (where N is the number of buses), whereas the methods presented in [9] and [10] require the tracing of $\binom{2N}{N}$ and $\frac{N \times S}{2}$ manifolds, respectively. Overall, the methodology proposed in this study provides a more robust approach for voltage stability assessment than existing methods, which typically yield only a pair of closely-located load-flow solutions or only a sub-set of all the Type-1 solutions.

ACKNOWLEDGMENT

We like to express sincere appreciation and deep gratitude to all participants in this work.

REFERENCES

[1] Chang, C.S. "Voltage Security Monitoring and Control in Electric Power Transmissi on Systems," Ph.D. Thesis, National Taiwan University, 1999.

[2] Mozina, C.J. "A shot in the dark," IEEE Ind. Appl. Vol. 14, pp. 45-52, 2008.

[3] Chang, C.S. "A Matrix-based VaR Model for Risk Identification in Power Supply Networks." Applied Mathematical Modeling, Vol. 35, pp. 4567-4574, 2011.

[4] Tamura, Y., Mori, H., Iwamoto, S. "Relationship between voltage instability and multiple load-flow solutions in electric power systems," IEEE Trans. Power App. Syst. Vol. 102, pp. 1115-1125, 1983.

[5] Alvarado, F.L., Dobson, I., Thomas, R.J., Hu, Y. "Computation of closest bifurcation in power systems," IEEE Trans. Power Syst. Vol. 9, pp. 918-928, 1994.

[6] Lu, J., Liu, C.W., Thorp, J.S. "New methods for computing a saddlenode bifurcation point for voltage stability analysis," IEEE Trans. Power Syst. Vol. 10, pp. 978-989, 1995.

[7] Dimitrovski, A., Tomsovic, K. "Boundary load flow solutions," IEEE Trans. Power Syst. Vol. 19, pp. 348-355, 2004.

[8] Guedes, R.B.L., Alberto, L.F.C., Bretas, N.G. "Power System Low-Voltage Solutions Using an Auxiliary Gradient System for Voltage Collapse Purposes," IEEE Trans. Power Syst. Vol. 20, pp. 1528-1537, 2005.

[9] Salam, F.M.A., Ni, L., Guo,S., Sun, X. "Parallel processing for the load flow of power systems: the approach and applications," In Proc. 28th Decision and Control Conf., Tampa, FL, pp. 2173-2178, Dec. 1989.

[10] Ma, W., Thorp, J.S. "An efficient algorithm to locate all the load-flow solutions," IEEE Trans. Power Syst., Vol. 8, pp. 1077-1083, 1993.

[11] Chiang, H.D., Dobson, I., Thomas, R.J., Thorp, J.S., Lazhar, F.A. "On voltage collapse in electric power systems," IEEE Trans. Power Syst. Vol. 5, pp. 601-611, 1990.

[12] Sauer, P.W., Pai, M.A. "Power system steady-state and the load-flow Jacobian," IEEE Trans. Power Syst. Vol. 5, pp. 1374-1383, 1990.

[13] Overbye, T.J., Klump, R.P. "Effective calculation of power system low-voltage solution," IEEE Trans. Power Syst. Vol. 11, pp. 75-82, 1996.

[14] Liu, C.W., Thorp, J.S. "A novel method to compute the closest unstable equilibrium point for transient stability region estimate in power system," IEEE Trans. Circuits Syst. I: Fundam. Theory Applicat. Vol. 44, pp. 630-635, 1997.

[15] Ting, T.O., Wong, K.P., Chung, C.Y. "Locating Type-1 Load Flow Solutions using Hybrid Evolutionary Algorithm," In Proceedings of the Fifth International Conference on Machine Learning and Cybernetics, pp. 4093-4098, Aug. 2006.

[16] Liu, C.W., Chang, C.S., Jiang, J.A. Yeh, G.H "Toward a CPFLOW-based algorithm to compute all the type-1 load-flow solutions in electric power systems," IEEE Trans. Circuits Syst. I: Fundam. Theory Applicat. Vol. 52, pp. 625-630, 2005.

[17] Guillemin, V., Pollack, A. Differential Topology, AMS Chelsea Publishing, 2010.

[18] Sotomayor, J. "Generic bifurcations of dynamic systems," Dynamical Systems, Peixoto, M.M. Ed., Academic Press: New York, 1973.

[19] Zhang, T., Wang, W. "Hopf bifurcation and bistability of a nutrient–phytoplankton–zooplankton model," Applied Mathematical Modeling, Vol. 36, pp. 6225-6235, 2012.

[20] Ma, Z.P. "Stability and Hopf bifurcation for a three-component reaction–diffusion population model with delay effect," Applied Mathematical Modeling , Vol. 37, pp. 5984-6007, 2013.

[21] Bairagi, N., Jana, D. "On the stability and Hopf bifurcation of a delay-induced predator-prey system with habitat complexity," Applied Mathematical Modeling, Vol. 35, pp. 3255-3267, 2011.

[22] Chow, S.N., Hale, J. Methods of Bifurcation Theory, Springer Verlag: New York, 1982.

[23] Allgower, E.L., Georg, K. "Introduction to Numerical Continuation Methods," Society for Industrial & Applied , 2003.

[24] Krauskopf, B., Osinga, H.M., Galan-Vioque, J. Numerical Continuation Methods For Dynamical Systems: Path Following And Boundary Value Problems, Springer Verlag, 2007.

[25] Soriano, M., Ordoñez Cabrera, M. "Continuation methods and condensing mappings," Nonlinear Analysis: Theory, Methods & Applications, Vol. 102, pp. 84-90, 2014.